Submitted to
32nd International Conference on High Energy Physics, ICHEP04, August 16, 2004, Beijing
Abstract: **6-0176**
Parallel Session **6**
www-h1.desy.de/h1/www/publications/conf/conf_list.html

Comparison at NLO between Predictions from QCD Fits to F_2^D and Diffractive Final State Observables at HERA

H1 Collaboration

Abstract

Diffractive parton distributions, obtained from a next-to-leading order QCD analysis of recent H1 inclusive diffractive deep-inelastic scattering data, are convoluted with QCD hard scattering matrix elements to predict cross sections at next-to-leading order for the diffractive production of jets and charm quarks off virtual photons. The predictions are compared with H1 measurements of dijet and D^* meson production cross sections in diffractive DIS. Within the experimental and theoretical uncertainties, the results are consistent with QCD factorization in diffractive DIS at NLO.

1 Introduction

Understanding the phenomenon of diffraction in hadronic interactions at high energies, where at least one of the beam hadrons remains intact (or dissociates to a small mass system Y carrying net proton quantum numbers) and loses only a small fraction $x_{I\!P}$ of its incident longitudinal momentum, remains one of the most important challenges in Quantum Chromodynamics (QCD). The ep collider HERA provides a unique possibility to study hard diffractive interactions in deep inelastic scattering (DIS) at large values of the photon virtuality Q^2.

Measurements of inclusive diffractive DIS at HERA have been used to extract *diffractive parton distributions* (diffractive pdf's) of the proton. If QCD factorization holds for diffractive DIS [1], these diffractive parton distributions are universal and may be used to predict the cross sections for exclusive hard diffractive DIS processes such as jet and heavy flavour production.

Recently, several new precision measurements of inclusive diffractive DIS have been presented by the H1 Collaboration at low [2], medium [3] and high [4] Q^2 values. Using the medium Q^2 data, and assuming a factorizing $x_{I\!P}$ dependence (see section 2.3), leading order (LO) and next-to-leading order (NLO) DGLAP QCD fits have been performed to determine diffractive parton distributions [3], updating previous results based on earlier data [5]. In this paper, these pdf's, interfaced to NLO QCD calculations, are used for comparisons with recent H1 measurements of D^* meson [6] and dijet [7] production cross sections in diffractive DIS. The result represents a test of QCD factorization in diffractive DIS at NLO.

2 Diffractive Parton Distributions

2.1 QCD factorization

QCD hard scattering factorization in diffractive DIS [1] suggests that in the leading $\log(Q^2)$ approximation, the cross section for the diffractive process $\gamma^* p \to Xp$ can be written in terms of convolutions of universal partonic cross sections $\hat{\sigma}^{\gamma^* i}$ with diffractive parton distributions p_i^D [8–10], representing probability distributions for a parton i in the proton under the constraint that the proton remains intact with particular values of 4-momentum transfer squared at the proton vertex t and $x_{I\!P}$. Thus, at leading twist,

$$\frac{\mathrm{d}^2\sigma(x,Q^2,x_{I\!P},t)^{\gamma^* p\to p'X}}{\mathrm{d}x_{I\!P}\,\mathrm{d}t} \;=\; \sum_i \int_x^{x_{I\!P}} \mathrm{d}\xi\; \hat{\sigma}^{\gamma^* i}(x,Q^2,\xi)\; p_i^D(\xi,Q^2,x_{I\!P},t)\;. \qquad (1)$$

The factorization formula is valid for large enough Q^2 and at fixed $x_{I\!P}$ and t. It also applies to the case of proton dissociation into a system of fixed small mass M_Y. The partonic cross sections $\hat{\sigma}^{\gamma^* i}$ are the same as for inclusive DIS and the diffractive parton distributions p_i^D, which are not known from first principles, should obey the DGLAP evolution equations.

Thus, analogously to inclusive DIS, the diffractive parton distributions can be constrained by experimental data by means of a DGLAP QCD fit to the inclusive diffractive DIS cross section. First analyses of such kind were performed in [5, 11, 12] based on measurements of the diffractive structure function F_2^D at HERA. The extracted parton distributions can then be used to predict diffractive final state cross sections, such as jet and heavy quark production, which allows the factorization theorem to be tested.

2.2 Regge Factorization

On top of the rigorous theoretical prescription represented by Eq. (1), an additional assumption is often made, namely that the shape of the diffractive parton distributions should be independent of $x_{I\!P}$ and t and their normalization controlled by Regge asymptotics [13]. The diffractive pdf's can then be factorized into a term depending only on $x_{I\!P}$ and t and a second term depending only on x (or $\beta = x/x_{I\!P}$) and Q^2:

$$p_i^D(x_{I\!P}, t, x, Q^2) = f_{I\!P/p}(x_{I\!P}, t) \cdot p_{i,I\!P}(\beta = x/x_{I\!P}, Q^2) \; . \tag{2}$$

This so-called *Regge* factorization assumption, in the literature often referred to as the *resolved pomeron* model, implies that the diffractive exchange can be treated as a quasi-real object with a partonic structure, given by parton distributions $p_{i,I\!P}(\beta, Q^2)$. The variable β then corresponds to the longitudinal momentum fraction of the diffractive exchange carried by the struck parton in the *pomeron*. The first term $f_{I\!P/p}(x_{I\!P}, t)$ (also called *pomeron flux factor*) represents the probability for scattering off a pomeron with particular values of $x_{I\!P}$ and t. It should be stressed that no proof in QCD exists for the assumption of Eq. (2). However, at the present level of precision it appears to be consistent with the data.

2.3 H1 Diffractive Parton Distributions

DGLAP QCD fits were performed in LO and NLO by the H1 Collaboration to the recent inclusive diffractive DIS data in [3], assuming Regge factorization. At high $x_{I\!P}$, a contribution from sub-leading meson ("reggeon") exchange was taken into account, such that the diffractive pdf's, integrated over t, are given by:

$$p_i^D(x_{I\!P}, \beta, Q^2) = f_{I\!P/p}(x_{I\!P}) p_{i,I\!P}(\beta, Q^2) + f_{I\!R/p}(x_{I\!P}) p_{i,I\!R}(\beta, Q^2) \; . \tag{3}$$

The pomeron and reggeon flux factors are given by

$$f_{\{I\!P,I\!R\}/p}(x_{I\!P}) = \int_{t_{cut}}^{t_{min}} \frac{e^{B_{\{I\!P,I\!R\}} t}}{x_{I\!P}^{2\alpha_{\{I\!P,I\!R\}}(t)-1}} \, \mathrm{d}t \; , \tag{4}$$

where $t_{cut} = -1.0 \text{ GeV}^2$, $|t_{min}|$ is the minimum kinematically allowed value of $|t|$ and the pomeron and reggeon trajectories are assumed to be linear functions of t:

$$\alpha_{\{I\!P,I\!R\}}(t) = \alpha_{\{I\!P,I\!R\}}(0) + \alpha'_{\{I\!P,I\!R\}} t \; . \tag{5}$$

The values of the parameters used in Eqs. 4 and 5 can be found in [3].

The pomeron parton distributions are composed of a light flavour singlet and a gluon distribution, which are evolved using the DGLAP equations, both in leading and in next-to-leading order. The strong coupling constant α_s was fixed by setting $\Lambda^{\overline{MS}}_{QCD} = 0.2$ GeV for 4 flavours, using the 1(2) loop expression for α_s at LO and NLO respectively, and the charm mass was set to $m_c = 1.5$ GeV. The meson pdf's were parameterised using a pion parton distribution function. The result of the fit is shown in Fig. 1. The shown uncertainty in the NLO pdf's includes the experimental uncertainty arising from the errors of the fitted data as well as the theoretical uncertainty, estimated by variations of m_c, Λ_{QCD} and the parameters used in the pomeron and reggeon flux factors.

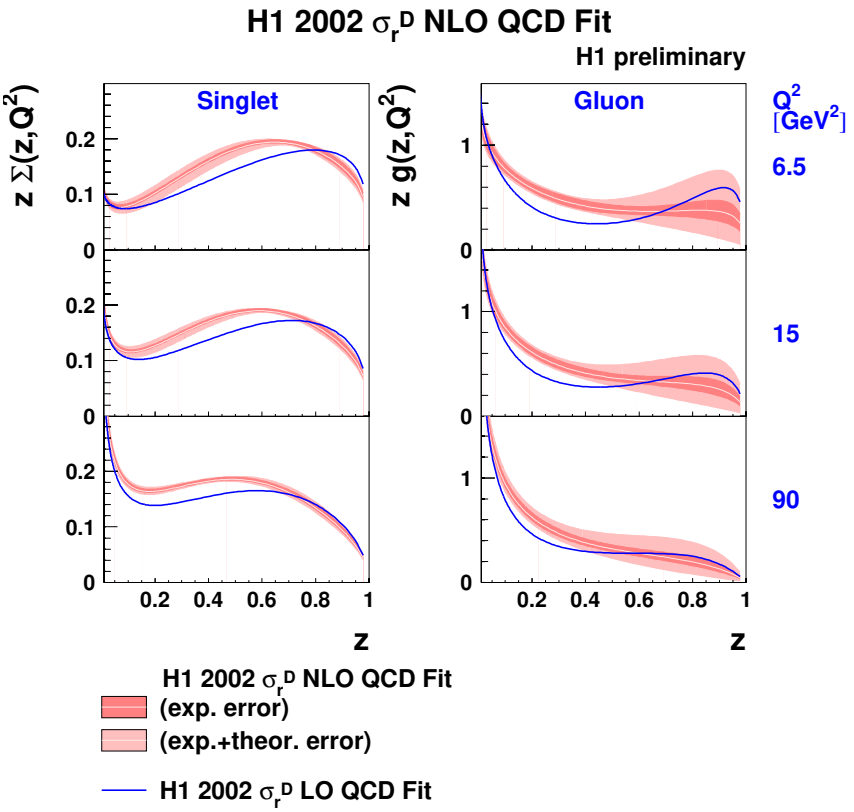

Figure 1: Quark singlet (left) and gluon (right) distribution functions at LO (lines) and NLO (bands) of the diffractive exchange at various values of Q^2, obtained from DGLAP QCD analyses of inclusive diffractive DIS data, from [3].

3 Diffractive DIS Dijet and D^* Cross Section Measurements

The NLO calculations presented in this paper are compared with recent H1 measurements of dijet and D^* meson production in diffractive DIS. An illustration of such processes at leading order QCD is shown in Fig. 2. In diffractive DIS, a photon with virtuality Q^2 emitted from the beam electron interacts with the proton, which loses only a small fraction $x_{I\!P}$ of its incident momentum and stays intact (or dissociates into a small mass system Y).

The longitudinal momentum fraction of the parton entering the hard scattering process relative to the diffractive exchange is labelled $z_{I\!P}$. In the hard scattering process, a pair of high transverse momentum (p_T) jets or heavy quarks is produced. The photon-proton centre-of-mass energy is W, which relates to the inelasticity y by $ys = Q^2 + W^2$, where s is the ep centre-of-mass energy. The invariant mass of the diffractively produced system X is M_X, and the invariant mass of the two partons emerging from the hard sub-process is given by $\sqrt{\hat{s}} = M_{12}$.

3.1 Diffractive Jet Production

H1 has measured differential cross sections for the diffractive production of dijets in DIS in [7]. Jets are defined using the CDF cone algorithm with cone radius $R = 1$. The kinematic range

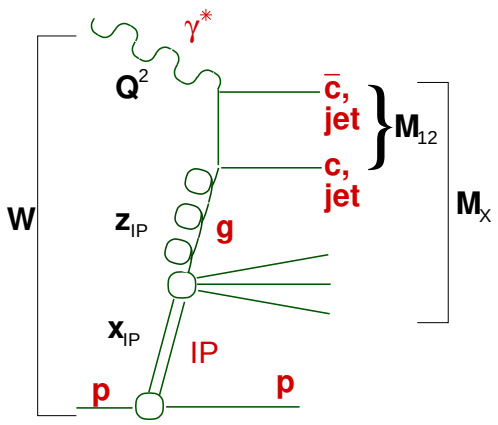

Figure 2: Diagram for jet or heavy quark pair production in the diffractive scattering of a virtual photon (γ^*), emitted by the beam electron, off the proton (p).

of the measurement is $4 < Q^2 < 80$ GeV^2, $0.1 < y < 0.7$, $x_{I\!P} < 0.05$, $|t| < 1.0$ GeV^2 and $M_Y < 1.6$ GeV. The transverse momenta and pseudorapidities of the two jets, which are searched for in the hadronic centre-of-mass frame, are required to be $p^*_{T,jet} > 4$ GeV and $-3 < \eta^*_{jet} < 0$, respectively.

Next-to-leading order dijet cross sections are not reliable in regions of phase space where the two jets have the same transverse momentum [14]. To facilitate a comparison of the cross sections [7] with NLO calculations, the data were corrected to the subsample where the transverse momentum of the first (second) jet is $p^*_{T,jet\ 1(2)} > 5(4)$ GeV. The correction is performed using leading order Monte Carlo programs, interfaced to parton showers [15] to approximate higher order QCD effects. Partons are fragmented to hadrons using the Lund string model [16]. The correction, defined as

$$c_{asym} = \frac{\sigma_{dijet}(p^*_{T,jet\ 1(2)} > 5(4)\ \text{GeV})}{\sigma_{dijet}(p^*_{T,jet\ 1(2)} > 4(4)\ \text{GeV})}\ , \tag{6}$$

is calculated using the RAPGAP program [17], interfaced to the "H1 fit 2" diffractive parton distributions [5], which yield a very good description of the dijet data in shape as well as normalization. Alternatively, the correction factors are evaluated using LEPTO [18], employing the "generalized area law" [19] model of soft colour interactions [20], which provides a poorer description of the shapes of the measured cross sections. Despite the different model assumptions, the correction factors obtained with the two programs are in good agreement. For the final correction, the average is taken as the central value and half of the difference is assumed as the uncertainty. The size of the correction is on average about 25% and it is found to vary smoothly as a function of kinematic variables other than $p^*_{T,jet}$.

3.2 Diffractive D^* Meson Production

Differential cross sections for the production of D^* mesons in diffractive DIS were measured by H1 [6]. The kinematic range of the data corresponds to $2 < Q^2 < 100$ GeV^2, $0.05 < y < 0.7$, $x_{I\!P} < 0.04$, $|t| < 1.0$ GeV^2 and $M_Y < 1.6$ GeV. The D^* mesons are identified through their

decay $D^{*\pm} \to (K^-\pi^+)\pi^+_{slow}$ (+c.c.). The transverse momenta and pseudo-rapidities of the D^* mesons in the laboratory frame are required to be $p_T(D^*) > 2$ GeV and $|\eta(D^*)| < 1.5$, respectively.

4 Next-to-leading Order QCD Calculations

QCD factorization in diffractive DIS [1] implies that the hard scattering cross section for the interaction of the virtual photon with a parton in a diffractive process is identical to the non-diffractive case. Therefore, state of the art programs which calculate fixed order partonic cross sections for dijet or heavy flavour production in ordinary DIS can be used also in the case of diffraction. The available programs calculate the cross section up to the next-to-leading order ($\mathcal{O}(\alpha_s^2)$) of perturbative QCD, using DGLAP evolution.

4.1 Diffractive Jet Production

To calculate diffractive dijet cross sections to NLO in QCD, the DISENT [21] program was used, as suggested in [22]. It was demonstrated in [23] that calculations using this program agree very well with the results from other programs. DISENT was interfaced to the diffractive parton distributions obtained in [3].

The cross section at a given fixed value of $x_{I\!P}$ and $t = 0$ is calculated by reducing the proton beam energy by a factor $x_{I\!P}$: $E_p = x_{I\!P} E_{p,nom.}$. Since the $x_{I\!P}$ and t dependences of the used diffractive pdf's factorize, the proton pdf's can be replaced by the pdf's of the diffractive exchange $p_{i,I\!P}(z, \mu^2)$, and the calculated cross sections are multiplied by the t-integrated flux factor $f_{I\!P/p}(x_{I\!P}) = \int \mathrm{d}t f_{I\!P/p}(x_{I\!P}, t)$. The partonic configurations are calculated for $t = 0$, such that kinematic effects of a finite value of t are neglected. Since the measured cross sections correspond to an interval in $x_{I\!P}$, the integration over $x_{I\!P}$ is approximated by summing up the results obtained for a set of suitably chosen $x_{I\!P}$ points ("$x_{I\!P}$ slicing"). The number of $x_{I\!P}$ points was chosen to ensure the calculation was of sufficient precision.

For the (N)LO calculations, the diffractive parton distributions are used in their respective version. The strong coupling constant α_s is set to the value assumed in the QCD fit from which the pdf's were extracted, using the corresponding 1(2)-loop expression and taking $\Lambda^{\overline{MS}}_{QCD} = 0.2$ GeV for 4 flavours. The renormalization scale is set to $\mu_r^2 = p_T^2$, where p_T^2 corresponds to the average transverse momentum of the two highest p_T partons in the Breit frame. The factorization scale is set to $\mu_f^2 = 40$ GeV^2, corresponding to the average p_T^2 of the two jets observed in the data, after the correction according to Eq. (6) has been applied. The parton configurations resulting from the calculations are subjected to the same jet algorithm as was used for the measured cross sections.

Since the calculations refer to jets of partons, whereas the measurements refer to jets of hadrons, the NLO calculations have to be corrected for the effects of hadronization. In the case of diffraction, these also include the definition of the diffractive kinematics, which at the hadron level are defined on the basis of the largest gap in rapidity in the hadronic final state, defining

two hadronic systems X and Y, from which $x_{I\!P}$, t and M_Y are calculated. The hadronization corrections, defined as

$$c_{had} = \frac{\sigma_{dijet}^{hadron}}{\sigma_{dijet}^{parton}} \, , \tag{7}$$

are determined using the leading order Monte Carlo RAPGAP, interfaced to the "H1 fit 2" diffractive pdf's. Since no alternative model of hadronization could be used, the correction factors are calculated using either parton showers (MEPS) or a colour dipole model (CDM) [24] to take higher order QCD effects into account. The size of the corrections is of the order of 10% and found to increase towards low values of p_T or $x_{I\!P}$. For the final corrections, the average of the values determined using MEPS and CDM is taken, and for its uncertainty half of the difference is taken with a conservative minimum uncertainty of 10% being assumed.

4.2 Diffractive D^* Meson Production

In [25], the HVQDIS [26] program, based on the NLO calculations for heavy quark production in DIS from [27], was extended to diffraction. The integration over $x_{I\!P}$ and t is performed numerically. Fragmentation of charm quarks is modeled using the standard Peterson fragmentation function [28].

The leading and next-to-leading order cross sections for diffractive D^* production are calculated using the (N)LO diffractive parton distributions from [3]. The prescription for α_s is the same as for the dijet calculations, as explained in section 4.1. For the central calculations, both the renormalization and the factorization scale are set to $\mu_r^2 = \mu_f^2 = Q^2 + 4m_c^2$. The charm mass is $m_c = 1.5$ GeV, the hadronization fraction is $f(c \to D^*) = 0.233$ and the parameter of the Peterson fragmentation function used is $\epsilon_{Pet.} = 0.078$.

5 Results

Comparisons at leading and next-to-leading order of the calculations based on diffractive parton distributions, obtained from QCD fits to inclusive diffractive DIS data in [3], and measured dijet production cross sections in diffractive DIS [7] are presented in Figs. 3-5, and for D^* production in diffractive DIS [6] in Figs. 6-7.

5.1 Diffractive Jet Production

In Fig. 3, the differential cross section for dijet production in diffractive DIS is presented as a function of $z_{I\!P}^{(jets)}$, an estimator for the longitudinal momentum fraction of the diffractive exchange entering the hard scattering. The data from [7] are corrected to asymmetric requirements on the minimum jet transverse momenta $p^*_{T,jet\ 1(2)} > 5(4)$ GeV, as explained in section 3.1. The inner error bars of the data points correspond to the statistical error, whereas the outer error bars represent the total uncertainty, including the systematic error as well as the uncertainty of the correction to asymmetric jet cuts, added in quadrature.

The data are compared with leading and next-to-leading order calculations using DISENT, interfaced to the diffractive pdf's from [3], obtained from a QCD analysis of inclusive diffractive DIS data. The uncertainty of the next-to-leading order calculation includes a variation of the renormalization scale $\mu_r^2 = p_T^2$ by factors of $1/4$ and 4 and the uncertainty in the hadronization corrections, which is added linearly to the renormalization scale uncertainty, the latter being typically of the order of 20%.

The leading order calculation clearly underestimates the measured cross section and is also unable to reproduce the observed shape of the $z_{I\!P}^{(jets)}$ distribution. The next-to-leading order corrections to the cross section are found to be large, exceeding a factor 2 on average. This is considered to be mostly due to the relatively small average transverse momentum of the jets. The size of the NLO correction decreases smoothly with increasing $p_{T,jet}$. The NLO calculation, corrected for hadronization effects, provides within the theoretical and experimental uncertainties a reasonable description of the shape and normalization of the measured cross section. The uncertainty of the NLO calculation does not include the uncertainty in the diffractive pdf's shown in Fig. 1. In particular, the uncertainty in the diffractive gluon distribution is comparatively large for $z > 0.5$.

In Fig. 4, the $z_{I\!P}^{(jets)}$ cross section is presented in four intervals of $Q^2 + p_T^2$ and also in four intervals of $x_{I\!P}$. In Fig. 5 differential dijet cross sections as a function of Q^2, the photon-proton centre-of-mass energy W, $\log_{10} x_{I\!P}$ and the average pseudo-rapidity $\langle\eta\rangle_{lab}^{jets}$ of the jets are shown. Also in these distributions, reasonable agreement is observed with the NLO calculations, corrected for hadronization, if the experimental and theoretical uncertainties are taken into account.

5.2 Diffractive D^* Meson Production

In Fig. 6, the differential cross section for D^* meson production in diffractive DIS, as measured in [6], is shown in bins of $z_{I\!P}$. The error bars of the data correspond to the sum of the statistical and systematic uncertainties, added in quadrature.

The data are compared with leading and next-to-leading order calculations using the diffractive version of HVQDIS, interfaced to the diffractive pdf's from [3]. The uncertainty of the NLO calculation corresponds to a variation of the renormalization scale $\mu_r^2 = Q^2 + 4m_c^2$ by factors of $1/4$ and 4 and variations of the charm quark mass within $m_c = 1.35 \ldots 1.65$ GeV and of the parameter of the Peterson fragmentation function within $\epsilon_{Pet.} = 0.035 \ldots 0.100$. Within the experimental and theoretical uncertainties, good agreement is observed between the data and the NLO calculations. The size of the NLO corrections is observed to be significantly smaller than in the case of diffractive dijet production.

The variation of the charm mass by ± 0.15 GeV changes the cross section by $\pm 12\%$, whereas choosing $\epsilon_{Pet.} = 0.035$ ($\epsilon_{Pet.} = 0.100$) changes the cross section by $+21\%$ (-7%). If the value of Λ_{QCD} at 4 flavours is changed by ± 30 MeV, the cross section changes by $\pm 5\%$ (not included in the error bands). If scales other than $\mu_r^2 = Q^2 + 4m_c^2$ are chosen for the renormalization scale, such as $Q^2 + m_c^2$, Q^2 or m_c^2, the cross section varies by $10 \ldots 15\%$.

In Fig. 7, differential cross sections are shown in bins of $\log_{10} Q^2$, the transverse momentum of the D^* in the hadronic centre-of-mass frame, p_{T,D^*}^*, the pseudo-rapidity of the D^* in the

laboratory frame, η_{D^*}, and of $x_{I\!P}$. Also for these distributions, good agreement is observed within the uncertainties.

6 Conclusions

Diffractive parton distributions determined by H1 using inclusive diffractive DIS data have been interfaced with next-to-leading order QCD calculations for the diffractive production of jets and heavy quarks in DIS. The calculations have been compared with recent H1 measurements of diffractive dijet and D^* meson production in DIS. Within the experimental and theoretical uncertainties, the calculations are found to be in good agreement with the data. The results are thus consistent with QCD factorization in deep-inelastic scattering as applied to diffraction at next-to-leading order.

Acknowledgements

We are grateful to the HERA machine group whose outstanding efforts have made this experiment possible. We thank the engineers and technicians for their work in constructing and maintaining the H1 detector, our funding agencies for financial support, the DESY technical staff for continual assistance and the DESY directorate for support and for the hospitality which they extend to the non-DESY members of the collaboration.

References

[1] J. Collins, *Phys. Rev.* **D 57** (1998) 3051 [erratum-ibid. **D 61** (2000) 019902].

[2] H1 Collaboration, "Measurement of the Diffractive Deep-Inelastic Scattering Cross Section at low Q^2", paper **981** submitted to the 31st Intl. Conference on High Energy Physics, ICHEP 2002, Amsterdam (2002).
(https://www-h1.desy.de/h1/www/publications/htmlsplit/H1prelim-02-112.long.html)

[3] H1 Collaboration, "Measurement and NLO DGLAP QCD Interpretation of Diffractive Deep-Inelastic Scattering at HERA", paper **980** submitted to the 31st Intl. Conference on High Energy Physics, ICHEP 2002, Amsterdam (2002).
(https://www-h1.desy.de/h1/www/publications/htmlsplit/H1prelim-02-012.long.html)

[4] H1 Collaboration, "Measurement of the Diffractive Reduced Cross Section $\sigma_r^{D(3)}$ at high Q^2", paper **090** submitted to the Intl. Europhysics Conference on High Energy Physics, EPS 2003, Aachen (2003).
(https://www-h1.desy.de/h1/www/publications/htmlsplit/H1prelim-03-011.long.html)

[5] H1 Collaboration, C. Adloff *et al.*, *Z. Phys.* **C 76** (1997) 613.

[6] H1 Collaboration, C. Adloff *et al.*, *Phys. Lett.* **B 520** (2001) 191.

[7] H1 Collaboration, C. Adloff *et al.*, *Eur. Phys. J.* **C 20** (2001) 29.

[8] L. Trentadue, G. Veneziano, *Phys. Lett.* **B 323** (1994) 201;
A. Berera, D. Soper, *Phys. Rev.* **D 50** (1994) 4328;
M. Grazzini, L. Trentadue, G. Veneziano, *Nucl. Phys.* **B 519** (1998) 394.

[9] W. Buchmüller, T. Gehrmann, A. Hebecker, *Nucl. Phys.* **B 537** (1999) 477.

[10] F. Hautmann, Z. Kunszt, D. E. Soper, *Nucl. Phys.* **B 563** (1999) 153;
F. Hautmann, D. E. Soper, *Phys. Rev.* **D 63** (2000) 011501.

[11] L. Alvero, J. C. Collins, J. Terron, J. J. Whitmore, *Phys. Rev.* **D 59** (1999) 074022.

[12] C. Royon, L. Schoeffel, J. Bartels, H. Jung, R. Peschanski, *Phys. Rev.* **D 63** (2001) 074004.

[13] G. Ingelman, P. Schlein, *Phys. Lett.* **B 152** (1985) 256.

[14] M. Klasen, G. Kramer, *Phys. Lett.* **B 366** (1996) 385;
S. Frixione, G. Ridolfi, *Nucl. Phys.* **B 507** (1997) 315;
B. Poetter, *Comp. Phys. Commun.* **113** (2000) 105.

[15] M. Bengtsson, T. Sjöstrand, *Z. Phys.* **C 37** (1988) 465.

[16] T. Sjöstrand, *Comp. Phys. Commun.* **82** (1994) 74.

[17] H. Jung, *Comp. Phys. Commun.* **86** (1995) 147.
(see also http://www.desy.de/∼jung/rapgap.html)

[18] A. Edin, G. Ingelman, J. Rathsman, *Comp. Phys. Commun.* **101** (1997) 108.

[19] J. Rathsman, *Phys. Lett.* **B 452** (1999) 364.

[20] A. Edin, G. Ingelman, J. Rathsman, *Phys. Lett.* **B 366** (1996) 371;
A. Edin, G. Ingelman, J. Rathsman, *Z. Phys.* **C 75** (1997) 57.

[21] S. Catani, M. H. Seymour, *Nucl. Phys.* **B 485** (1997) 29 [erratum-ibid. **B510** (1997) 503].

[22] F. Hautmann, JHEP **0210** (2002) 025.

[23] C. Duprel, T. Hadig, N. Kauer, M. Wobisch, "Comparison of next-to-leading order calculations for jet cross-sections in deep inelastic scattering" in A. Doyle, G. Grindhammer, G. Ingelman, H. Jung (eds.), Proc. of the Workshop on Monte Carlo Generators for HERA Physics, DESY-PROC-1999-02 (1999).

[24] G. Gustafson, *Phys. Lett.* **B 175** (1986) 453;
G. Gustafson, U. Petterson, *Nucl. Phys.* **B 306** (1988) 746;
B. Andersson, G. Gustafson, L. Lönnblad, U. Petterson, *Z. Phys.* **C 43** (1989) 625;
B. Andersson, G. Gustafson, L. Lönnblad, *Nucl. Phys.* **B 339** (1990) 393.

[25] L. Alvero, J. C. Collins, J. J. Whitmore, "Tests of factorization in diffractive charm production and double pomeron exchange", hep-ph/9806340.

[26] B. W. Harris, J.Smith, *Phys. Rev.* **D 57** (1998) 2806.

[27] B. W. Harris, J.Smith, *Nucl. Phys.* **B 452** (1995) 109;
B. W. Harris, J.Smith, *Phys. Lett.* **B 353** (1995) 535 [erratum-ibid. **B359** (1997) 423].

[28] C. Peterson, D. Schlatter, I. Schmitt, P.M. Zerwas, *Phys. Rev.* **D 27** (1983) 105.

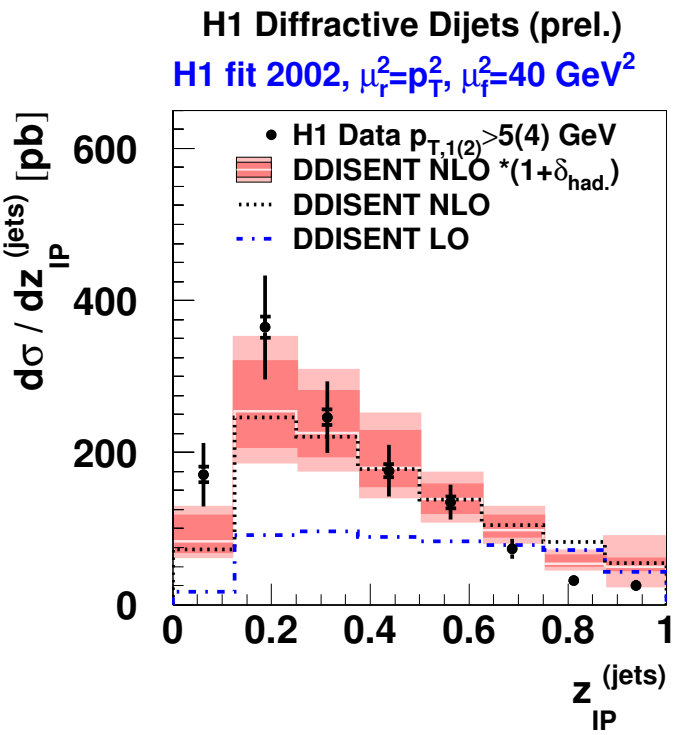

Figure 3: Differential cross section for dijet production in diffractive DIS from [7] (points), corrected to asymmetric cuts on the jet transverse momentum $p^*_{T,1(2)} > 5(4)$ GeV, shown as a function of $z_{I\!P}^{(jets)}$, an estimator for the longitudinal momentum fraction of the diffractive exchange entering the hard process. The data are compared with predictions based on the (N)LO diffractive parton distributions from [3], using $\mu_r^2 = p_T^2$ and $\mu_f^2 = 40$ GeV^2. Shown are predictions obtained with DISENT (using the $x_{I\!P}$ slicing technique, see text) at leading order QCD (blue, dash-dotted line), at next-to-leading order QCD (black, dotted line) and at next-to-leading order including hadronization corrections (central line of error band). The inner error band represents the renormalization scale uncertainty, while the outer band also includes the uncertainty in the hadronization corrections, added linearly.

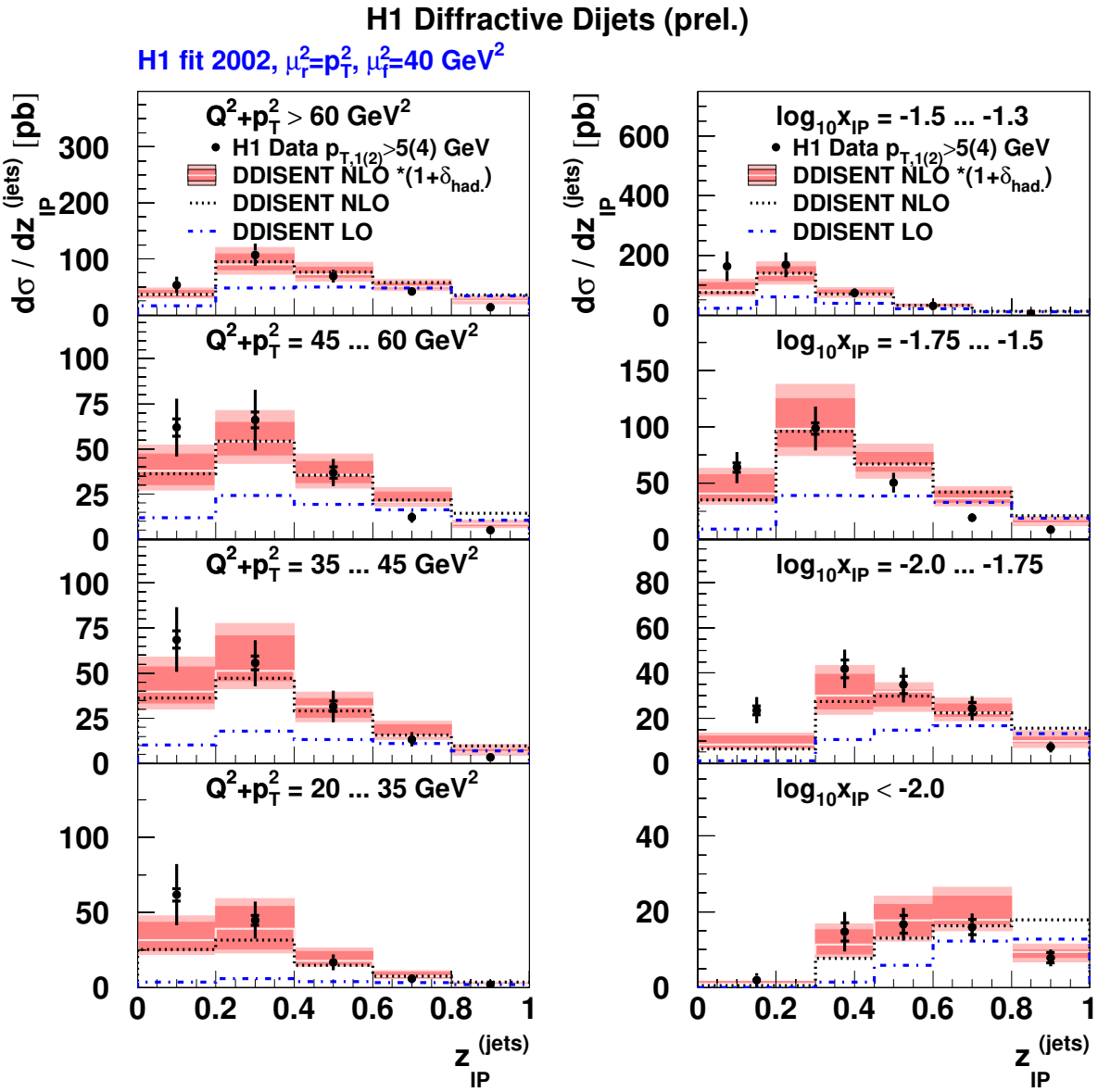

Figure 4: Differential cross section for dijet production in diffractive DIS from [7] (points), corrected to asymmetric cuts on the jet transverse momentum $p^*_{T,1(2)} > 5(4)$ GeV, shown as a function of $z_{I\!P}^{(jets)}$, an estimator for the momentum fraction of the longitudinal momentum fraction of the diffractive exchange entering the hard process, for four intervals of $Q^2 + p_T^2$ (left) and $x_{I\!P}$ (right), respectively. The data are compared with predictions based on the (N)LO diffractive parton distributions from [3], using $\mu_r^2 = p_T^2$ and $\mu_f^2 = 40$ GeV^2. Shown are predictions obtained with DISENT (using the $x_{I\!P}$ slicing technique, see text) at leading order QCD (blue, dash-dotted line), at next-to-leading order QCD (black, dotted line) and at next-to-leading order including hadronization corrections (central line of error band). The inner error band represents the renormalization scale uncertainty, while the outer band also includes the uncertainty in the hadronization corrections, added linearly.

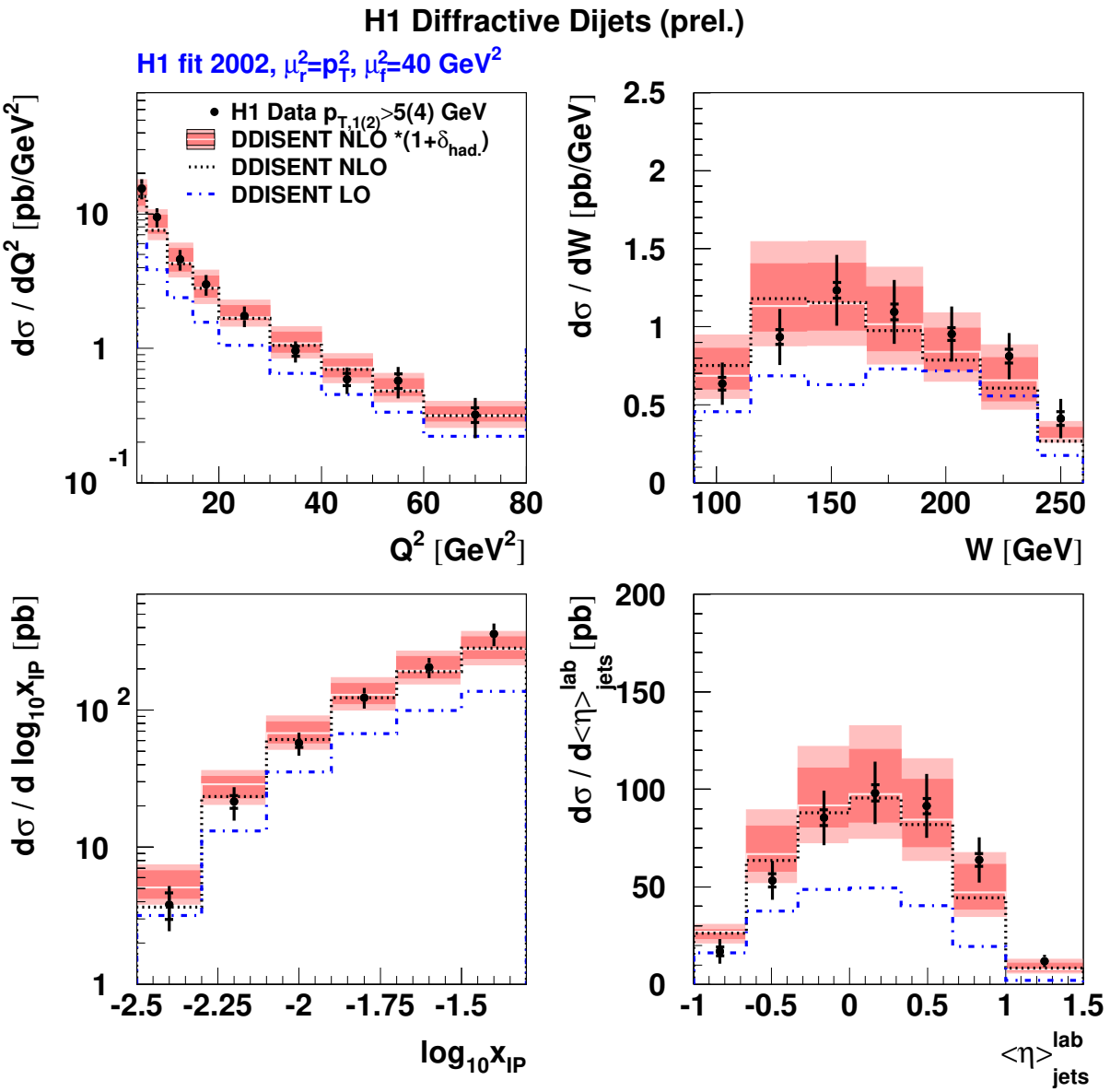

Figure 5: Differential cross section for dijet production in diffractive DIS from [7] (points), corrected to asymmetric cuts on the jet transverse momentum $p^*_{T,1(2)} > 5(4)$ GeV, shown as a function of the photon virtuality Q^2, the photon-proton centre-of-mass energy W, the longitudinal proton momentum fraction taken by the diffractive exchange $x_{I\!P}$ and the average pseudorapidity of the jets $\langle\eta\rangle^{lab}_{jets}$. The data are compared with predictions based on the (N)LO diffractive parton distributions from [3], using $\mu_r^2 = p_T^2$ and $\mu_f^2 = 40$ GeV^2. Shown are predictions obtained with DISENT (using the $x_{I\!P}$ slicing technique, see text) at leading order QCD (blue, dash-dotted line), at next-to-leading order QCD (black, dotted line) and at next-to-leading order including hadronization corrections (central line of error band). The inner error band represents the renormalization scale uncertainty, while the outer band also includes the uncertainty in the hadronization corrections, added linearly.

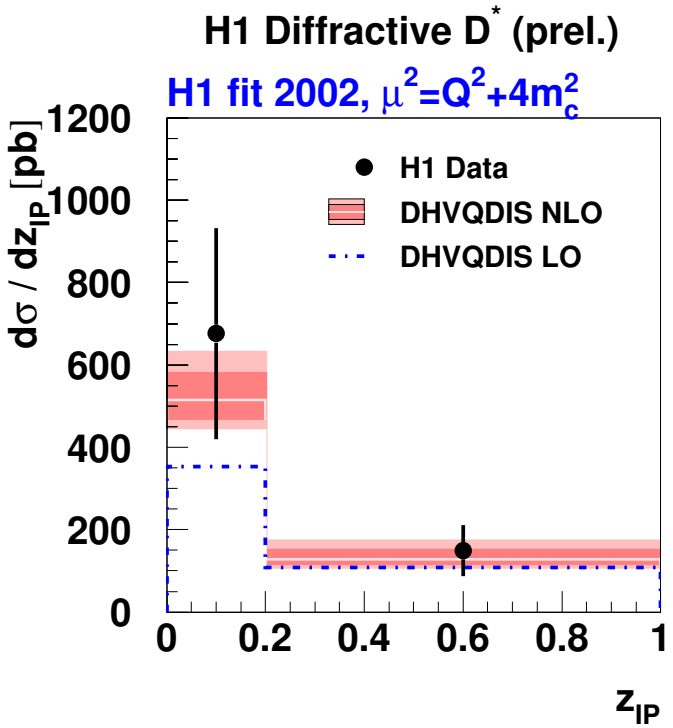

Figure 6: Differential cross sections for D^* meson production in diffractive DIS from [6] (points), shown as a function of $z_{I\!P}$, an estimator for the longitudinal momentum fraction of the diffractive exchange entering the hard process. The data are compared with predictions based on the (N)LO diffractive parton distributions from [3], using $\mu_r^2 = \mu_f^2 = Q^2 + 4m_c^2$. Shown are predictions obtained with the diffractive version of HVQDIS at leading order QCD (blue, dash-dotted line) and at next-to-leading order QCD (central line of error band). The inner error band represents the renormalization scale uncertainty, while the outer error band shows the total uncertainty, which includes variations of the charm mass in the range $m_c = 1.35 \ldots 1.65$ GeV and of the parameter of the Peterson fragmentation function $\epsilon_{Pet.} = 0.035 \ldots 0.100$, added in quadrature.

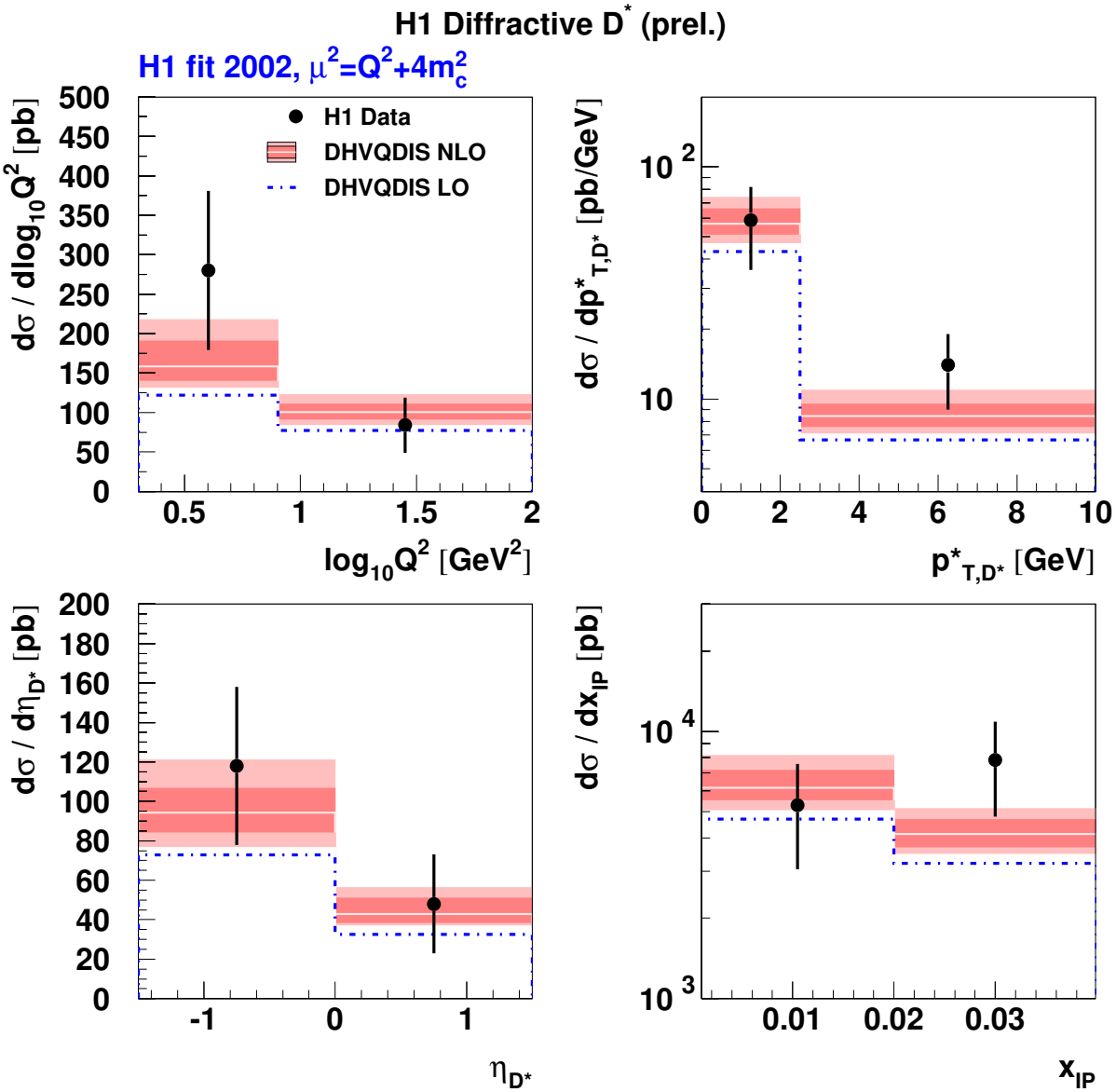

Figure 7: Differential cross sections for D^* meson production in diffractive DIS from [6] (points), shown as a function of the photon virtuality Q^2, the transverse momentum of the D^* in the $\gamma^* p$ centre-of-mass frame p^*_{T,D^*}, the pseudo-rapidity of the D^* in the laboratory frame η_{D^*} and the longitudinal proton momentum fraction taken by the diffractive exchange $x_{I\!P}$. The data are compared with predictions based on the (N)LO diffractive parton distributions from [3], using $\mu_r^2 = \mu_f^2 = Q^2 + 4m_c^2$. Shown are predictions obtained with the diffractive version of HVQDIS at leading order QCD (blue, dash-dotted line) and at next-to-leading order QCD (central line of error band). The inner error band represents the renormalization scale uncertainty, while the outer error band shows the total uncertainty, which includes variations of the charm mass in the range $m_c = 1.35 \ldots 1.65$ GeV and the parameter of the Peterson fragmentation function $\epsilon = 0.035 \ldots 0.100$, added in quadrature.